Available online at www.sciencedirect.com
SCIENCE DIRECT®
Journal of Molecular Graphics and Modelling 22 (2003) 173–181
Journal of Molecular Graphics and Modelling
www.elsevier.com/locate/JMGM

Molecular determinants of LXRα agonism

Minmin Wang [a,*,1], Jeffrey Thomas [b,1], Thomas P. Burris [c], Jeffrey Schkeryantz [a], Laura F. Michael [b]

[a] *Department of Discovery Chemistry Research and Technologies, Eli Lilly & Company, Lilly Research Laboratories, DC 1513, Indianapolis, IN 46285, USA*
[b] *Department of Cardiovascular Research, Eli Lilly & Company, Indianapolis, IN 46285, USA*
[c] *Department of Gene Regulation, Eli Lilly & Company, Indianapolis, IN 46285, USA*

Received 27 March 2003; received in revised form 23 June 2003; accepted 24 June 2003

Abstract

Liver X receptors (LXRs) are nuclear receptors that participate in the regulation of cholesterol, bile acid, and glucose metabolism. Despite the identification of the natural oxysterol and nonsteroidal ligands for LXRα, little is known about the structure of the LXRα ligand-binding domain (LBD). We constructed a three-dimensional (3D) homology model of the LBD of LXRα based on the crystal structure of the retinoic acid receptor γ (RARγ) and all-*trans* retinoic acid complex. We combined molecular modeling and classical structure–function techniques to define the interactions between the LBD and three structurally diverse ligands, 22(*R*)-hydroxycholesterol (22RHC), *N*-(2,2,2-trifluoro-ethyl)-*N*-[4-(2,2,2-trifluoro-1-hydroxy-1-trifluoromethyl-ethyl)-phenyl]-benzenesulfonamide (T0901317) and (3-{3-[(2-chloro-3-trifluoromethyl-benzyl)-(2,2-diphenyl-ethyl)-amino]-propoxy}-phenyl)-acetic acid (GW3965). Sixteen individual amino acid point mutations were made in the predicted ligand-binding cavity of the LBD, and each of these mutant receptors was assessed for their ability to be activated by these three ligands. The majority of individual mutations resulted in lack of activation by all three ligands. Two residues were identified that resulted in a significant increase in basal activity while retaining responsiveness to the ligands. Interestingly, a number of residues were identified that appear to be selective in their response to a particular ligand, indicating that these three ligands recognize distinct structural components within the ligand-binding cavity. These data, together with our docking study, enable us to identify the amino acids that coordinate the interaction of both steroidal and non-steroidal ligands in the ligand-binding pocket of LXRα.

Keywords: Ligand-binding domain; Liver X receptors; Single-point mutation; Atherosclerosis

1. Introduction

As a component of cell membranes and as a precursor to steroid and bile acid biosynthesis, cholesterol is essential for homeostasis. Yet, a balance between cholesterol biosynthesis and utilization must be maintained since high levels of circulating cholesterol can lead to atherosclerotic lesion formation. Indeed, cholesterol and oxysterol metabolites regulate cholesterol homeostasis by acting both in feedback regulation of the cholesterol biosynthetic pathway and in feedforward regulation of cholesterol catabolism via bile acid synthesis. Primary mediators of such regulation are the nuclear receptors, LXRα (NR1H3) and LXRβ (NR1H2), which are receptors of oxysterols that increase expression of cholesterol 7α-hydroxylase (Cyp7A1), the rate-limiting enzyme in bile acid synthesis [1]. Activation of LXRs also directly promotes the transcription of genes that are involved in cholesterol efflux from peripheral tissues, such as ATP-binding cassette (ABC) transporter ABCA1, ABCG1 and apolipoprotein E, as well as genes that regulate lipogenesis, such as sterol response element binding protein 1 and fatty acid synthase [2–6]. More recently, a role for LXRs in the regulation of glucose metabolism and inflammation has been defined [7,8]. Thus, modulation of LXR activities by ligands could result in treatments for cardiovascular disease, dyslipidemia, diabetes, as well as inflammatory disorders. Towards understanding the consequences of pharmacological activation of LXRs in vitro and in vivo, several natural and synthetic ligands have been identified. 22(*R*)-hydroxycholesterol, 24(*S*)-hydroxycholesterol and 24(*S*),25-epoxycholesterol are naturally-occurring agonists for LXR that bind at physiological concentrations and likely serve as the endogenous modulators of LXR activities [1,9,10]. Potent, synthetic LXR agonists, such as T0901317

* Corresponding author. Tel.: +1-317-433-9621; fax: +1-317-276-5431.
E-mail address: wang_minmin@lilly.com (M. Wang).
[1] These authors contributed equally to this work.

1093-3263/$ – see front matter © 2003 Elsevier Inc. All rights reserved.
doi:10.1016/S1093-3263(03)00159-1

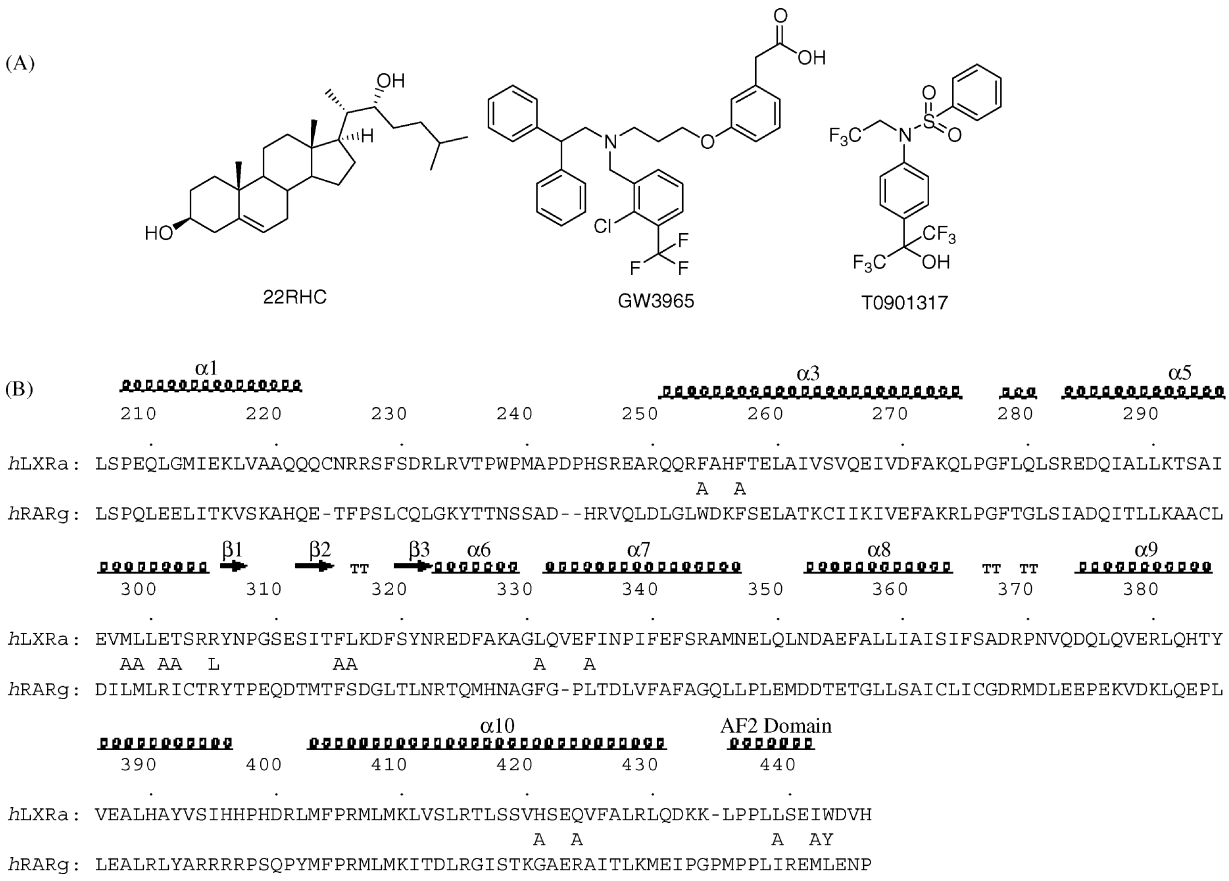

Fig. 1. (A) Chemical structure of 22RHC, T0901317 and GW3965. (B) Sequence alignment and secondary structure of LXRα LBD. Point mutations are marked below the corresponding residues.

[4] and GW3965 [11] (Fig. 1A), recently have been developed and utilized to study the effects of LXR activation in vivo. Major fatty acid biosynthetic genes were unexpectedly induced following acute treatment of mice and hamsters with T0901317, a finding that revealed SREBP1 as a direct target gene of LXR [4–6]. However, as proof that modulation of LXR activity may ameliorate cholesterol accumulation in the vasculature, despite increases in lipid synthesis, chronic treatment of two animal models of atherosclerosis (ApoE$^{-/-}$ and LDLR$^{-/-}$ mice) with GW3965 significantly reduced aortic lesion area [12]. A crystal structure of an agonist-bound nuclear receptor ligand-binding domain undoubtedly enables the rational design of compounds with agonistic activities. Thus far, a crystal structure of agonist-bound LXR LBD has not been reported. Here, in its absence, we have constructed a homology model of the LXRα LBD bound either by 22RHC, GW3965 or T0901317. Structure–activity relationships (SAR) between the amino acids of the LBD and the various compounds were elucidated by site-directed mutagenesis of selected amino acid residues followed by transcriptional activation analysis in the presence of each compound. We have discerned that while some mutations in the LBD abolish transcriptional induction by all of the tested ligands, other mutations reveal amino acid-selective contacts with the ligands that result in divergent potentiation activities. Our model identifies specific amino acid residues that are obligatory for transcriptional activation as well as amino acids that divergently modulate LBD activity based on ligand-specific interactions.

2. Experimental procedures

2.1. Homology model and ligand docking

All calculations were performed on a Silicon Graphics Indigo O2 R12000 (Silicon Graphics Inc.) workstation. The three-dimensional (3D) homology model for the LBD of *h*LXRα was constructed by using the automated comparative homology modeling program, Modeler [13], as implemented in InsightII2000 (Accelrys Inc., San Diego, 2000). Unlike the conventional homology modeling scheme with time consuming stages of core region identification and loop region building, Modeler uses a unique probability density functions (PDFs) to transfer the spatial restraints from the template to the target proteins. The individual restraints are assembled into a single molecular probability density function (MPDF) and optimized to give 3D coordinates for the

target protein. The initial position of LBD was determined by masking off the zf-C4 domain in protein family (Pfam) search of nuclear receptors. The crystal structure of retinoic acid γ (RARγ, PDB code 2lbd) was chosen as template based on the high identity score (36.1%) between the two sequences. The sequence alignment was generated using BLOSUM62 scoring matrix with gap opening penalty of 10 and gap extension penalty of 1 [14]. Portions of overhanging sequence on LXRα LBD were cut during the model building process. Two models were built with high level of optimization for the conserved regions with high level of optimization in the loop regions also. None of the hydrogen atoms are built in the homology model. The model with lowest −ln(PDF) value was selected as the final model and validated with protein health check in Quanta98 (Accelrys Inc., San Diego, 1999) to ensure no bad conformation on backbones and side chains in the ligand-binding pocket. The final homology model for LXRα LBD is comprised of amino acids 206–446. 22RHC, T0901317, and GW3965 were docked in an initial locus, based on the known positioning of all-*trans* retinoic acid (ATRA) in the RARγ–ATRA complex. Subsequently a CHARMm-based flexible docking protocol CDocker was utilized to fully optimize the conformation and orientation of the compounds in LXRα LBD [15–17]. This novel docking protocol utilizes a combination of simulated annealing and CHARMm-based energy function to search for local minimum. The receptor was kept rigid during the docking process. The side-chain rotamers of W443 and I295 were manually adjusted to accommodate GW3965, without disrupting the overall protein fold. For each ligand, 10 'best-docked' structures were examined to comply with the SAR trends in literature [10,11]. The volume of the ligand-binding pocket was estimated by castP [18].

2.2. Site-directed mutagenesis

Single amino acid point mutations were made in pM-*h*LXRα LBD expression (pM LXRα LBD; aa 162–447, accession number NM_005693) plasmid using QuikChange® site-directed mutagenesis kit following the manufacturer's protocol (Strategene, La Jolla, CA). PAGE-purified complementary oligonucleotide primer sets were purchased from Qiagen Operon (Almeda, CA). The sense strand oligonucleotide sequences are as follows:

F254A GGCCCGTCAGCAGCGCGCTGCCCACTTCACTGAGC
F257A GCAGCGCTTTGCCCACGCCACTGAGCTGGCCATC
M298A GACCTCTGCGATCGAGGTGGCGCTTCTGGAGACATCTCG
L299A GCGATCGAGGTGATGGCTCTGGAGACATCTCGGAGG
E301A CGAGGTGATGCTTCTGGCGACATCTCGGAGGTACAACC
T302A GCTTCTGGAGGCATCTCGGAGGTACAACC
R305L GCTTCTGGAGACATCTCGGCTGTACAACCCTGGG
F315A CACTTCCTCAAGGATGCCAGTTATAACCGGGAAG
L316A GGAGTGAGAGTATCACCTTCGCCAAGGATTTCAGTTATAACCGGG
L331A GGAAGACTTTGCCAAAGCAGGGGCGCAAGTGGAATTCATCAA
F335A GCAGGGCTGCAAGTGGAAGCCATCAACCCCATCTTCG
H421A GGACCCTGAGCAGCGTCGCCTCAGAGCAAGTGTTTGC
Q424A GCAGCGTCCACTCAGAGGCAGTGTTTGCACTGCGTCTGC
L439A GCTCCCACCGCTGGCCTCTGAGATCTGGGATGTGC
I442A GCTGCACATCCCAGGCCTCAGAGAGCAGCGGTGGG
W443Y CACCGCTGCTCTCTGAGATCTACGATGTGCACGAATG

Mutagenesis was confirmed by sequence analysis.

2.3. Cell culture and transient transfections

For transient transfection of HEK293 cells, 6×10^3 cells were plated into each well of a 96-well dish. Each well of transfection contained 25 ng 5XUAS-luciferase reporter (pG5*luc*) and 25 ng of either wild-type or mutated pM LXRα LBD plasmid using Fugene 6 reagent (Roche, Indianapolis, IN). Each chimeric protein was assessed for the ability to transactivate a Gal4-responsive luciferase reporter plasmid in a dose-responsive manner to each LXRα ligand (0.001–1 μM T0901317, 0.01–10 μM GW3965, and 0.1–30 μM 22RHC). Luciferase activity at each dose concentration was measured in triplicate. The percent increase or decrease of activity was determined by comparison to activation that was elicited by the wild-type Gal4-LXRα protein at the most efficacious dose. Luciferase activity was measured using standard substrate reagents (BD Biosciences, San Diego, CA).

2.4. Immunoblot analysis

HEK293 cells were transfected with the various pM LXRα LBD mutated plasmids. After 48 h, cells were lysed with 1% NP-40 lysis buffer, and 40 μg of total cellular proteins were separated by SDS-PAGE. Immunoblotting was performed using anti-GAL4 antibody following manufacturer's protocol (Santa Cruz Biotechnology, Santa Cruz, CA).

3. Results

Despite the identification of the natural oxysterol and non-steroidal ligands for LXRα, little is known about the 3D

structure of the LXRα LBD in the presence of ligands. In an effort to characterize the molecular interactions between the oxysterol, 22(*R*)-hydroxycholesterol (22RHC), and the non-steroidal ligands T0901317 and GW3965, we developed a novel homology model of the LXRα LBD with each ligand docked. RARγ was selected as template based on the high identity score between the amino acid sequences of these two receptors. The sequence identity between the LBDs of *h*RARγ and *h*LXRα is 36.1%, and the sequence alignment is shown in Fig. 1B. The amino acid sequences spanning 1–205 that encode the activation domain 1, the DNA binding domain, and hinge domain of LXRα were excluded from the homology model.

Overall, the size of the LXRα ligand-binding pocket as defined by homology modeling is ∼1400 Å^3, which is nearly the size of the PPAR ligand-binding domains (estimated about 1100–1400 Å^3 for PPARγ, PPARδ and PPARα) and is much larger than the retinoid receptor ligand-binding domains (600–800 Å^3) for RARs or RXRs. These volumes are consistent with the size of the compounds that are reported to bind to the different receptor subfamilies. The overall homology model of LXRα is similar to the canonical conformation of all previously reported agonist-bound LBD of nuclear receptors [19]. The LBD consists of 10 helices arranged in antiparallel helix sandwich, whereby the bona fide ligand-binding pocket is composed by helices 3, 5, 7, 10 and the AF2 domain. In addition, a three-stranded antiparallel β sheet is situated in the core of the LBD. The RMSD for 236 Cα atom pairs between the RARγ template and the homology model is 0.45 Å. The largest deviation of Cα trace between RARγ and LXRα is found in the region of 241–246. Various residues within the binding pocket were selected for mutagenesis analysis in order to determine the contribution of each amino acid residue in ligand-binding (Fig. 1B).

Using a chimeric Gal4-LXRα LBD plasmid template, a total of sixteen amino acid substitutions were made that included residues within the helices 3, 5, 7, 10 and the AF2 domain (Fig. 1B). Each chimeric protein was assessed for the ability to transactivate a Gal4-responsive luciferase reporter plasmid in a dose-responsive manner to each LXRα ligand (0.001–1 μM T0901317, 0.01–10 μM GW3965, and 0.1–30 μM 22RHC). The percent increase or decrease of activity was determined by comparison to activation that was elicited by the wild-type Gal4-LXRα protein at the most efficacious dose (Fig. 2A). Notably, the potency of each compound remained constant when each mutant receptor was tested (data not shown). Relative expression of each chimera was confirmed by Western blot analysis (Fig. 2B).

For each ligand, the 10 best-docked modes were saved and compared with the mutagenesis results and SAR trends that have been reported in the literature [10,11]. Table 1 summarizes the compliance of the 10 possible binding modes for each ligand with the mutagenesis results, and the final binding modes were selected accordingly.

Based on our refined homology model and our experimental findings, we propose a different orientation for the binding modality of 22RHC in the LXRα LBD, as compared to the previous reported pharmacophore model [20]. We propose an interaction between the C22 hydroxyl group of 22RHC with the Nε of R305 (Fig. 3B), namely, because the substitution R305L abrogates transcriptional activation by 22RHC (Fig. 2A). This orientation also validates the retention of activity for 24(*S*)-hydroxycholesterol (24SHC), 24(*S*),25-epoxycholesterol and 24-ketocholesterol through the maintenance of a hydrogen bond with R305.

(A)

	T0901317	GW3965	22R(HC)
Wild Type	100%	100%	100%
F254A	-99%	-99%	-88%
F257A	-94%	-88%	-81%
M298A	-26%	-95%	-86%
L299A	-5%	+48%	+135%
E301A	-60%	-64%	-89%
T302A	+56%	+84%	+411%
R305L	+ 5%	-53%	-88%
F315A	+125%	+30%	+437%
L316A	+476%	-26%	-65%
L331A	-92%	-98%	-93%
F335A	-96%	-83%	-72%
H421A	-99%	+42%	-96%
Q424A	-58%	-53%	-96%
L439A	-99%	-99%	-90%
I442A	-99%	-99%	-92%
W443Y	-96%	-20%	-92%

(B)

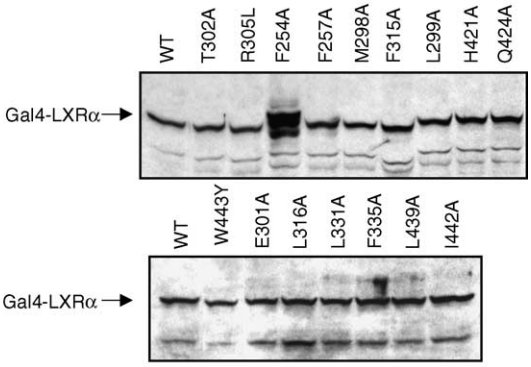

Fig. 2. (A) Transcriptional activities of various LXR-LBD mutants in the presence of T0901317, GW3965, or 22RHC. HEK293 cells were co-transfected with the Gal4-responsive luciferase plasmid (pG5*luc*) and an expression plasmid encoding wild-type or mutated LXRα-LBD fused to the GAL4 DNA-binding domain (pM LXRα-LBD). Cells were treated either with a dose-response of T0901317, GW3965, or 22RHC (see Section 2). Following 24 h of treatment, cells were lysed and firefly luciferase was measured. The percent increase or decrease of activity was determined by comparison to activation that was elicited by the wild-type Gal4-LXRα protein at the most efficacious dose. (B) HEK293 cells were transfected with the various pM LXRα LBD mutated plasmids as indicated. After 48 h, cells were lysed, and 40 μg of total cellular proteins were separated by SDS-PAGE. Immunoblotting was performed using anti-GAL4 antibody.

Table 1
Summary of 10 docked conformers for each ligand in compliance with the single-point mutation results

	22RHC										T0901317										GW3965									
	1	2	3	**4**	5	6	7	8	9	10	1	2	3	4	5	6	7	8	9	**10**	**1**	2	3	4	5	6	7	8	9	10
F254A	✓	✓	✓	✓	×	×	✓	✓	×	×	✓	✓	✓	✓	✓	✓	✓	✓	✓	✓	✓	✓	✓	✓	✓	✓	✓	✓	✓	✓
F257A	✓	✓	✓	✓	✓	✓	✓	✓	✓	✓	✓	✓	✓	✓	✓	✓	✓	✓	✓	✓	✓	✓	✓	✓	✓	✓	✓	✓	✓	✓
M298A	✓	✓	✓	✓	✓	✓	✓	✓	✓	✓	✓	✓	✓	✓	✓	✓	✓	✓	✓	✓	✓	✓	✓	✓	✓	✓	✓	✓	✓	✓
L299A	×	✓	×	✓	✓	✓	×	×	×	×	×	×	×	×	×	×	×	✓	✓	✓	✓	✓	✓	✓	✓	✓	✓	×	×	×
E301A	✓	✓	✓	✓	✓	✓	✓	×	✓	✓	×	×	✓	✓	✓	×	×	✓	×	✓	✓	✓	✓	✓	✓	✓	✓	✓	✓	×
T302A	✓	✓	✓	✓	✓	✓	✓	×	✓	✓	×	×	×	×	✓	×	×	✓	×	✓	✓	✓	✓	✓	✓	✓	✓	✓	✓	×
R305L	×	✓	✓	✓	×	×	×	✓	✓	✓	✓	✓	✓	✓	✓	×	×	✓	×	✓	✓	✓	✓	✓	✓	✓	✓	✓	✓	×
F315A	✓	✓	✓	✓	✓	×	✓	×	✓	✓	✓	✓	×	×	✓	✓	✓	✓	✓	✓	✓	✓	✓	✓	✓	✓	✓	✓	✓	×
L316A	✓	×	✓	✓	✓	✓	×	✓	✓	✓	×	×	×	✓	×	×	×	×	×	✓	✓	✓	×	✓	×	✓	✓	×	✓	✓
L331A	✓	✓	✓	✓	✓	✓	✓	✓	×	×	✓	✓	✓	✓	✓	✓	✓	✓	✓	✓	✓	✓	✓	✓	✓	✓	✓	✓	✓	✓
F335A	✓	✓	✓	✓	✓	✓	✓	✓	×	×	✓	✓	✓	✓	✓	✓	✓	×	✓	✓	✓	✓	✓	✓	✓	✓	✓	✓	✓	✓
H421A	✓	✓	✓	✓	✓	✓	✓	✓	✓	✓	✓	✓	✓	✓	✓	✓	✓	✓	✓	✓	✓	✓	✓	✓	✓	✓	✓	✓	✓	✓
Q424A	✓	✓	✓	✓	×	✓	✓	✓	×	×	×	×	×	×	✓	×	×	×	✓	✓	✓	✓	✓	✓	✓	✓	✓	✓	✓	✓
L439A	✓	✓	✓	✓	×	×	✓	✓	✓	✓	✓	✓	✓	✓	✓	✓	✓	✓	✓	✓	✓	✓	×	×	×	×	✓	✓	✓	✓
I442A	✓	✓	✓	✓	×	✓	✓	✓	✓	✓	×	×	×	×	×	×	×	×	×	✓	✓	✓	×	×	✓	×	✓	×	✓	✓
W443Y	✓	✓	✓	✓	×	×	✓	✓	✓	✓	✓	✓	✓	✓	✓	✓	✓	✓	✓	✓	✓	✓	✓	×	✓	✓	✓	✓	✓	×

Symbol (✓) indicates that the docking mode consistent with the mutation result; (×) indicates a conflict between the docking mode and the mutation result.

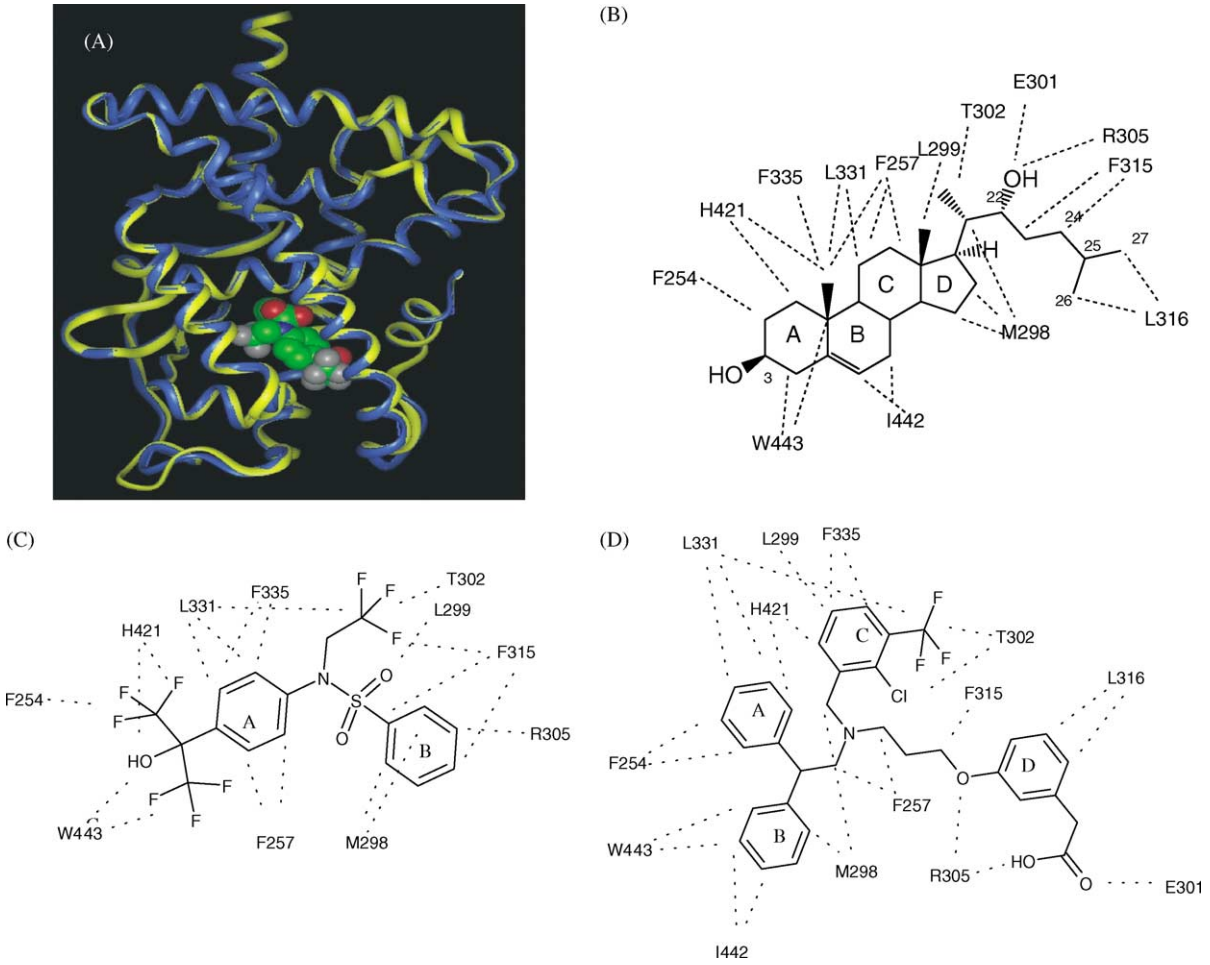

Fig. 3. (A) The superimposition of LXRα (yellow) and RARγ (blue). T09001317 is presented in the binding pocket of LXRα. Schematic drawing showing the interaction between the protein and the ligand molecules: 22RHC (B); T0901317 (C); and GW3965 (D).

The distance from the hydroxyl group, the epoxide oxygen and the oxygen of 24-ketone are all within 3.5 Å of Nε of R305. Spencer et al. could not explain the activity of 20(*S*)-hydroxycholesterol (20SHC) by the pharmacophore hypothesis in which the hydroxyl/or epoxide of the oxysterols forming a hydrogen bond with W443. In our model, the distance from the C20 hydroxyl of 20SHC to the backbone carbonyl of M298 is 2.5 Å, thus explaining the observed 20SHC activity. The potency of 24(*R*)-hydroxycholesterol and 24(*R*),25-epoxycholesterol may result from a hydrogen bond between the oxygen and the backbone amine of L316. Binding of 25-hydroxycholesterol may be mediated through a hydrogen bond between C25 hydroxyl and the backbone C=O of L260. R305L also causes a significant decrease in the transcriptional response to GW3965 in this study, suggesting that the ether oxygen of GW3965 could accept the hydrogen bond from R305. By contrast, T0901317 does not offer a hydrogen bond donor or acceptor that could participate in the interaction with R305, and the response of R305L to T0901317 is not as pronounced as compared to GW3965 and 22RHC.

The contributions of five additional polar residues within the LBD also were examined by structure–function analysis. A T302A substitution resulted in a universal increase in efficacy of the Gal4-LXRα response to all three ligands where the most significant increase occurred in response to 22RHC. In an earlier report by Vivat et al. [21], a constitutively active RXRα mutant, F313A, was described. Based on alignment of RXRs and LXRs (Fig. 4), the residue in LXRα that corresponds to RXRα F313 is T302. Our modeling shows that LXRα T302 is surrounded by hydrophobic residues F257 (α3), I313 (β2), F315 (loop), F326 (α6), I339 (α7), and the distance measured from CG2 of I313 to OG1 of T302 is 2.8 Å. Based on evidence of C–H···O hydrogen bonds in nuclear receptors [22], we suggest that T302 forms a weak hydrogen bond with I313 and that T302A acts as a constitutively active mutant by this mechanism. In contrast, E301A caused a universal decrease of response to all three ligands. The side chain of E301 is within hydrogen bond distance either to the C22 hydroxyl group of 22RHC or to the carboxylate oxygen of GW3965; therefore, the decrease of the response is likely due to the loss of hydrogen bond interaction. We cannot exclude the possibility that the residue participates in a charge network formed by N225, Q221, S264 and R305. Alternatively, the E301A mutant could cause the inability of the chimera to effectively recruit a ligand-dependent coactivator, such as SRC1.

*h*LXRα	302	TSRRY	306	…	438	LLSEIW 443
*h*LXRβ	316	TARRY	320	…	453	LLSEIW 458
*h*RXRα	313	FSHRS	317	…	450	FLMEML 455
*h*RXRβ	384	FSHRS	388	…	521	FLMEML 526
*h*RXRγ	314	FSHRS	318	…	451	FLMEML 456
*h*RARα	273	ICTRY	277	…	409	LIQEML 414
*h*RARβ	266	ICTRY	270	…	402	LIQEML 407
*h*RARγ	275	ICTRY	279	…	411	LIREML 416

Fig. 4. Partial sequence alignment of LXRs, RXRs and RARs.

Q424A also causes a universal decrease in transcriptional response to each of the three compounds. In our current model, Q424 is located on helix 10, and the side chain of the residue does not appear to participate in hydrogen bond interaction with any of the ligands tested. Rather, the modeling result showed that Q424 forms a hydrogen bond with Q332 on helix 7. We hypothesize that the hydrogen bond between H10 and H7 is important for appropriate folding of the LBD.

H421A demonstrated ligand-dependent transcriptional activity in the functional assay. The mutant increases the LXRα LBD transcriptional response to GW3965 while 22RHC and T0901317 produced decreased responses, indicating the residue is important for ligand specificity. Our model shows the imidazole ring of H421 is buried within a cluster of three phenyl rings in GW3965, and the increase in H421A responsiveness implies that partially replacing the aromatic clustering, as in GW3965, may be favorable for the interaction with LBD. In our model, the vector from the methyne group on H421 points towards the π clouds of the di-substituted A-ring of T0901317, forming edge-to-face interaction (Fig. 3C); therefore, the complete loss of transcriptional response to T0901317 was expected for the H421A mutant.

We also explored the contributions of 11 hydrophobic residues of LXRα in the interaction with steroid and nonsteroid ligands. Seven mutants, F254A, F257A, M298A, L331A, F335A, L439A and I442A, decrease LXRα LBD transcriptional responses by 70–99% for all three compounds, demonstrating common space occupied by all structural classes. Based on the model, these seven residues likely form two hydrophobic pockets. The major pocket includes side chains from F254, F257, L331 and F335 and the minor side pocket includes M298, L439 and I442. These two pockets are boarded by W443 and H421.

Mutations W443Y, L299A and L316A revealed ligand-specific interaction of these residues in the transcriptional assay. In agreement with Spencer et al. [20] we observed complete loss of transcriptional activation by 22RHC in the presence of a W443Y substitution. W443 has been proposed to serve as a hydrogen bond donor to the hydroxyl or carbonyl groups on C17 side chain the oxysterols; however, the conclusion is not exclusive since the hydroxyl group of tyrosine could also act as a hydrogen bond donor. Accordingly, we suggest an orientation whereby W443 participates in a hydrophobic interaction with 22RHC. Indeed, the loss of transcriptional induction by W443Y in the presence of 22RHC and T0901317 likely results from a van der Waals collision when W443 is replaced with tyrosine. Mutation of W443Y did not result in as dramatic of a reduction in

transcription in the presence of GW3965. Based on our docking model, we propose an edge-to-face interaction between the A ring of GW3965 with W443 and F257 of the LBD (Fig. 3D); hence, the slight difference in GW3965-mediated transactivation between the W443Y mutant and the wild-type LBD may be caused by the redistribution of π-electron clouds on the aromatic ring. The L299A mutation increased the transcriptional response both to GW3965 and to 22RHC but had almost no impact on T0901317-mediated induction. Since L299 participates in hydrophobic stacking with H421, replacing the *iso*-propyl side chain with smaller methyl group may provide flexibility to H421 and offer alternative binding mode for the ligand. We were unable to determine whether the ligand affinity changes for the mutant, but the impact is more likely scaffold-specific. The L316A mutation caused a surprising increase in T0901317 efficacy and a moderate decrease in GW3965- and 22RHC-induced transcription. The decrease of activity for GW3965 and 22RHC was expected since L316 is within van der Waals contact distance of the gem-di-methyl at C25 of 22RHC and the aromatic C–H on the D-ring of GW3965 in our model. However, we are unable to explain the increased activity of T0901317 since L316 is not in direct contact with the compound. It may be possible, though, that T0901317 increases the efficiency of co-factor recruitment in the context of the L316A mutant. The ligand-dependent biocharacter of these three residues indicates that it is not necessary for diverse structural classes to occupy the same space for the functional activity and that transfer of SAR trends across scaffolds may require more detailed study.

F268 in LXRβ has been shown to be important both in ligand-binding and in cellular response to oxysterol [23]. This finding substantiates our results because the corresponding residue of LXRβ F268 is F254 in LXRα (Fig. 4). The F254A mutant of LXRα abolished transcriptional responses to all three classes of compounds. Similarly, Chen et al. reported that mutation of L469A on PPARγ ablated both cofactor interaction and ligand-binding [24]. Based on our sequence alignment (Fig. 4), the corresponding residue in LXRα is L439, and this residue is conserved among most nuclear receptors (data not shown). When L439 was mutated, we also observed a universal loss of transactivation response for all three compound classes. This provides further evidence that residues homologous to L439 are critical for ligand-binding across all nuclear receptors.

Surprisingly, the F315A mutation is the only hydrophobic residue substitution that caused a universal increase of transcriptional responses for all three compounds, ranging from 30% for GW3965 to 437% for 22RHC. Our model predicts that the side chain of F315 has broad interaction with C17, C23 and C24 of 22RHC. Since this residue is conserved between LXRs, RARs, and RORs, one could speculate that mutation of this analogous residue in any of these receptors would result in a receptor with substantial elevation in basal transcriptional activity.

4. Discussion

Despite improved clinical care and widespread use of lipid-lowering drugs, such as statins, coronary heart disease (CHD) remains the leading cause of death in the United States, and currently an estimated 12 million persons in the US are living with CHD [25]. Statins, inhibitors of 3-hydroxy-3-methylglutaryl coenzyme A reductase, are the most effective class of LDL-cholesterol lowering drugs. Although LDL cholesterol-lowering is the current primary target of therapy, effective treatment of CHD necessitates increasing low HDL cholesterol levels [26]. One promising molecular target for raising HDL cholesterol is the nuclear receptor, LXR. Potent LXR agonists activate genes involved not only in HDL accumulation, but also in catabolism of cholesterol to bile acids, in regulation of several genes important for reverse cholesterol transport from peripheral tissues, and in cholesterol excretion into bile or intestinal lumen. The battery of LXR target genes mediating these effects includes Cyp7A1, ABCA1, ABCG1, apolipoprotein E, LPL, CETP, ABCG5, and ABCG8 [1–3,27–32]. Thus, understanding the molecular requirements for modulating LXR activity in vivo may lead to exciting new pharmacological interventions for patients with low HDL cholesterol.

LXR potentiates target gene expression, in part, through ligand-dependent receptor activation. Yet, a crystal structure describing the LXRα LBD has not been reported to date. Here, rather, we leveraged the high sequence identity between LXRα and RARγ to construct a homology model for the LXRα LBD. Three binding modes were proposed following site-directed mutagenesis and SAR using three distinct chemical entities, which enabled dissection of the amino acids and chemical forces that mediate ligand-binding and transcriptional activation by LXRα. Unlike other nuclear pharmacophore models that utilize a single class of structurally-related compounds for SAR and modeling, we broadened our study to include three structurally-distinct molecules to probe the LXRα LBD. In so doing, we believe that our homology model of the LXRα LBD is more comprehensive and predictive of the actual LXRα LBD structure and of the amino acids that are involved in coordinating ligands.

Whether the LXRα LBD amino acids that we have studied are involved in various diseases processes such as atherosclerosis, diabetes, and Alzheimer's disease remains to be determined. However, single nucleotide polymorphisms (SNPs) of genes can be identified from several publicly available SNP databases by in silico methods. Indeed, we found candidate SNPs within the coding region (cSNPs) of LXRα that have been described previously [33]. *rs1131379* and *rs1050945* are two described SNPs located within the LXRα LBD. Another SNP *rs2279238* that corresponds to position 99 of the protein sequence also has been described. However, all three of these SNPs are synonymous changes. Whether these or other cSNPs are associated with differential LXR pharmacology and whether an association between

hypercholesterolemic or diabetic cohorts and certain cSNPs can be drawn will be of great interest. As SNPs in the LBD of LXR continue to emerge, we anticipate that our model will aid the prediction of the differential LXR activities and pharmacology. In silico screening of myriad chemical entities using this model, coupled to receptor activation measurement, may ultimately lead to more chemical tools for studying the in vivo activities of LXR and its ability to modulate HDL cholesterol levels. Additionally, high-resolution cocrystal structures of the LXRα LBD could facilitate the design of drugs for a variety of diseases, such as atherosclerosis, diabetes, and inflammation.

5. Note

While this manuscript was in review, the co-crystal structures of LXRβ with 24(*S*),25-epoxycholesterol and T09001317 was released by JBC (in press) on 7 May 2003 [34]. The nonsteroidal agonist, T0901317, in the co-crystal structure has the same orientation as predicted by our methodology. However, the co-crystal structure revealed a different binding mode for oxysterol whereby the epoxide oxygen acts as hydrogen bond acceptor of the imidazole of H435. The crystal binding mode for 22RHC agrees with the third out of the 10 best solutions found in this docking study (Table 1, 22RHC, column 3), however, the orientation was rejected due to disagreement with the structure–function analysis of the mutant L299A. The induced transcriptional response by 22RHC on L299A mutant led to the hypothesis of a bulky group in the neighborhood, and based on existing knowledge of other sterols that have been crystallized with hormone receptors, we selected the presented mode as the most favorable binding mode. The possibility exists that some of the functional changes observed in L299A is not through direct interaction with the ligand, which could be corroborated with a high-resolution crystal structure.

Acknowledgements

We are grateful to Dr. Chen Su for the search of SNPs and Drs. Jon Erickson, James H. Wikel, Timothy Grese, and John Munroe for insightful discussions and suggestions.

References

[1] J.M. Lehmann, S.A. Kliewer, L.B. Moore, T.A. Smith-Oliver, B.B. Oliver, et al., Activation of the nuclear receptor LXR by oxysterols defines a new hormone response pathway, J. Biol. Chem. 272 (1997) 3137–3140.
[2] A. Venkateswaran, B.A. Laffitte, S.B. Joseph, P.A. Mak, D.C. Wilpitz, et al., Control of cellular cholesterol efflux by the nuclear oxysterol receptor LXR alpha, Proc. Natl. Acad. Sci. U.S.A. 97 (2000) 12097–12102.
[3] P.A. Mak, B.A. Laffitte, C. Desrumaux, S.B. Joseph, L.K. Curtiss, et al., Regulated expression of the apolipoprotein E/C-I/C-IV/C-II gene cluster in murine and human macrophages. A critical role for nuclear liver X receptors alpha and beta, J. Biol. Chem. 277 (2002) 31900–31908.
[4] J.R. Schultz, H. Tu, A. Luk, J.J. Repa, J.C. Medina, et al., Role of LXRs in control of lipogenesis, Genes Dev. 14 (2000) 2831–2838.
[5] T. Yoshikawa, H. Shimano, M. Amemiya-Kudo, N. Yahagi, A.H. Hasty, et al., Identification of liver X receptor–retinoid X receptor as an activator of the sterol regulatory element-binding protein 1c gene promoter, Mol. Cell Biol. 21 (2001) 2991–3000.
[6] J.J. Repa, G. Liang, J. Ou, Y. Bashmakov, J.M. Lobaccaro, et al., Regulation of mouse sterol regulatory element-binding protein-1c gene (SREBP-1c) by oxysterol receptors, Genes Dev. 14 (2000) 2819–2830.
[7] G. Cao, Y. Liang, C.L. Broderick, B.A. Oldham, T.P. Beyer, et al., Antidiabetic action of a liver X receptor agonist mediated by inhibition of hepatic gluconeogenesis, J. Biol. Chem. 278 (2003) 1131–1136.
[8] S.B. Joseph, A. Castrillo, B.A. Laffitte, D.J. Mangelsdorf, P. Tontonoz, Reciprocal regulation of inflammation and lipid metabolism by liver X receptors, Nat. Med. 9 (2003) 213–219.
[9] B.A. Janowski, P.J. Willy, T.R. Devi, J.R. Falck, D.J. Mangelsdorf, An oxysterol signalling pathway mediated by the nuclear receptor LXR alpha, Nature 383 (1996) 728–731.
[10] B.A. Janowski, M.J. Grogan, S.A. Jones, G.B. Wisely, S.A. Kliewer, et al., Structural requirements of ligands for the oxysterol liver X receptors LXRalpha and LXRbeta, Proc. Natl. Acad. Sci. U.S.A. 96 (1999) 266–271.
[11] J.L. Collins, A.M. Fivush, M.A. Watson, C.M. Galardi, M.C. Lewis, et al., Identification of a nonsteroidal liver X receptor agonist through parallel array synthesis of tertiary amines, J. Med. Chem. 45 (2002) 1963–1966.
[12] S.B. Joseph, E. McKilligin, L. Pei, M.A. Watson, A.R. Collins, et al., Synthetic LXR ligand inhibits the development of atherosclerosis in mice, Proc. Natl. Acad. Sci. U.S.A. 99 (2002) 7604–7609.
[13] A. Sali, T.L. Blundell, Comparative protein modelling by satisfaction of spatial restraints, J. Mol. Biol. 234 (1993) 779–815.
[14] http://www.arabidopsis.org/blast/blastoptions.html.
[15] M. Vieth, J.D. Hirst, B.N. Dominy, H. Daigler, C.L. Brooks III, Assessing search strategies for flexible docking, J. Comput. Chem. 19 (1998) 1623–1631.
[16] M. Vieth, J.D. Hirst, A. Kolinski, C.L. Brooks III, Assessing energy functions for flexible docking, J. Comput. Chem. 19 (1998) 1612–1622.
[17] M. Vieth, D.J. Cummins, DoMCoSAR: a novel approach for establishing the docking mode that is consistent with the structure–activity relationship. Application to HIV-1 protease inhibitors and VEGF receptor tyrosine kinase inhibitors, J. Med. Chem. 43 (2000) 3020–3032.
[18] http://cast.engr.uic.edu/cgi-bin/cast1/index.pl.
[19] J.M. Wurtz, W. Bourguet, J.P. Renaud, V. Vivat, P. Chambon, et al., A canonical structure for the ligand-binding domain of nuclear receptors, Nat. Struct. Biol. 3 (1996) 206.
[20] T.A. Spencer, D. Li, J.S. Russel, J.L. Collins, R.K. Bledsoe, et al., Pharmacophore analysis of the nuclear oxysterol receptor LXRalpha, J. Med. Chem. 44 (2001) 886–897.
[21] V. Vivat, C. Zechel, J.M. Wurtz, W. Bourguet, H. Kagechika, et al., A mutation mimicking ligand-induced conformational change yields a constitutive RXR that senses allosteric effects in heterodimers, EMBO J. 16 (1997) 5697–5709.
[22] B.P. Klaholz, D. Moras, C–H···O hydrogen bonds in the nuclear receptor RAR—a potential tool for drug selectivity, Structure 10 (2002) 1197–1204.
[23] F. Urban Jr., G. Cavazos, J. Dunbar, B. Tan, P. Escher, et al., The important role of residue F268 in ligand binding by LXRbeta, FEBS Lett. 484 (2000) 159–163.
[24] S. Chen, B.A. Johnson, Y. Li, S. Aster, B. McKeever, et al., Both coactivator LXXLL motif-dependent and -independent interactions

are required for peroxisome proliferator-activated receptor gamma (PPARgamma) function, J. Biol. Chem. 275 (2000) 3733–3736.
[25] CDC decline in deaths from heart disease and stroke—United States, 1900–1999, MMWR (1999) 649–656.
[26] R.S. Rosenson, The rationale for combination therapy, Am. J. Cardiol. 90 (2002) 2K–7K.
[27] D.J. Peet, S.D. Turley, W. Ma, B.A. Janowski, J.M. Lobaccaro, et al., Cholesterol and bile acid metabolism are impaired in mice lacking the nuclear oxysterol receptor LXR alpha, Cell 93 (1998) 693–704.
[28] S. Murthy, E. Born, S.N. Mathur, F.J. Field, LXR/RXR activation enhances basolateral efflux of cholesterol in CaCo-2 cells, J. Lipid Res. 43 (2002) 1054–1064.
[29] B.A. Laffitte, J.J. Repa, S.B. Joseph, D.C. Wilpitz, H.R. Kast, et al., LXRs control lipid-inducible expression of the apolipoprotein E gene in macrophages and adipocytes, Proc. Natl. Acad. Sci. U.S.A. 98 (2001) 507–512.
[30] Y. Zhang, J.J. Repa, K. Gauthier, D.J. Mangelsdorf, Regulation of lipoprotein lipase by the oxysterol receptors, J. Biol. Chem. 18 (2001) 18.
[31] Y. Luo, A.R. Tall, Sterol upregulation of human CETP expression in vitro and in transgenic mice by an LXR element, J. Clin. Invest. 105 (2000) 513–520.
[32] J.J. Repa, K.E. Berge, C. Pomajzl, J.A. Richardson, H. Hobbs, et al., Regulation of ATP-binding cassette sterol transporters ABCG5 and ABCG8 by the liver X receptors alpha and beta, J. Biol. Chem. 277 (2002) 18793–18800.
[33] http://www.ncbi.nlm.nih.gov/SNP/index.html.
[34] S.P. Williams, R.K. Bledsoe, J.L. Collins, S. Boggs, M.H. Lambert, et al., X-ray crystal structure of the liver X receptor ligand binding domain: regulation by a histidine-tryptophan switch, J. Biol. Chem. (2003).